Direct search for features in the primordial bispectrum

Stephen Appleby [a,b], Jinn-Ouk Gong [b,c,*], Dhiraj Kumar Hazra [b,d], Arman Shafieloo [e,f], Spyros Sypsas [b,g]

[a] School of Physics, Korea Institute for Advanced Study, Seoul 02455, Republic of Korea
[b] Asia Pacific Center for Theoretical Physics, Pohang 37673, Republic of Korea
[c] Department of Physics, Postech, Pohang 37673, Republic of Korea
[d] AstroParticule et Cosmologie & Paris Centre for Cosmological Physics, Université Paris Diderot, Paris 75205, France
[e] Korea Astronomy and Space Science Institute, Daejeon 34055, Republic of Korea
[f] University of Science and Technology, Daejeon 34113, Republic of Korea
[g] Departamento de Física, Universidad de Chile, Santiago 837.0415, Chile

A B S T R A C T

We study features in the bispectrum of the primordial curvature perturbation correlated with the reconstructed primordial power spectrum from the observed cosmic microwave background temperature data. We first show how the bispectrum can be completely specified in terms of the power spectrum and its first two derivatives, valid for any configuration of interest. Then using a model-independent reconstruction of the primordial power spectrum from the Planck angular power spectrum of temperature anisotropies, we compute the bispectrum in different triangular configurations. We find that in the squeezed limit at $k \sim 0.06$ Mpc^{-1} and $k \sim 0.014$ Mpc^{-1} there are marginal 2σ deviations from the standard featureless bispectrum, which meanwhile is consistent with the reconstructed bispectrum in the equilateral configuration.

1. Introduction

Recent observational progress on the temperature anisotropies of the cosmic microwave background (CMB) has made primordial inflation [1] the most promising candidate to describe the early universe. Being an effective description at a relatively low energy embedded in an ultraviolet complete theory, it is natural to expect that the inflationary Lagrangian contains substructure which prevents otherwise smooth evolution of the universe during the entire inflationary epoch [2]. The resulting features in the primordial correlation functions imply enhanced interactions, giving rise to a unique observational window into the unknown physics of the parent theory.

Over the previous decade it has been shown that the primordial power spectrum reconstructed from the observed CMB data allows for the existence of features with roughly 5% modulations in the amplitude [3–5]. Although there is no high confidence detection beyond the smooth power-law form of the primordial power

spectrum, the search for features remains tantalizing due to their potential ability to rule out a large class of inflationary scenarios. Furthermore, the existence of features in the power spectrum implies features also in higher order correlation functions. This suggests a compelling way to look for features in the bispectrum by using its correlation with the power spectrum.

In this article, using the primordial power spectrum reconstructed directly from the Planck temperature data [5], we search for scales and triangular configurations at which we would expect non-trivial signals in the bispectrum. The method described in this work, being both fast and accurate, provides an ideal platform to search for correlated features in the primordial bispectrum [6,7].

2. Bispectrum in terms of power spectrum

The explicit correlation between the power spectrum of the curvature perturbation $\mathcal{R}$ and its bispectrum was first elucidated in [8], where the features are sourced by a non-trivial speed of sound c_s. This is motivated from an effective single field description of inflation when heavy degrees of freedom are systematically integrated out [9]. Given that $|1 - c_s^{-2}| \ll 1$, we can explicitly find the leading contributions to the bispectrum $B_{\mathcal{R}}$ [8]. Moreover, it was noted in [10] that the correlation between correlation func-

tions can be further extended in the context of the generalized slow roll formalism (GSR) [11] from the relation [12]

$$\log\left(\frac{1}{f^2}\right) = \int_0^\infty \frac{dk}{k} m(-k\tau) \log \mathcal{P}_\mathcal{R}(k),\tag{1}$$

where $f = f(\log \tau) \equiv -2\pi\tau z$, with $z^2 \equiv 2a^2\epsilon m_{\mathrm{Pl}}^2/c_s$, $\epsilon \equiv -\dot{H}/H^2$ and $d\tau \equiv c_s dt/a$, is the GSR fundamental function and $m(x) \equiv 2\left[x^{-1} - x^{-1}\cos(2x) - \sin(2x)\right]/\pi$. Then, the "source" of the power spectrum $g_P \equiv (f'' - 3f')/f$ with $f' \equiv df/d\log\tau$ can be written in terms of $\mathcal{P}_\mathcal{R}$ and its first two derivatives, i.e. $n_\mathcal{R}$ and $\alpha_\mathcal{R}$.

On totally general grounds, the bispectrum is specified by additional information on the source of the bispectrum g_B [13], which is obtained from the cubic order action [14]. In the effective field theory viewpoint [15], the action at each order is specified by a set of mass scales M_n^4, so that at quadratic order M_2^4 determines c_s, while at cubic order M_3^4 is to be additionally specified, in principle, as an independent coupling. This is materialized as the bispectrum source g_B, which is not generically written in terms of the power spectrum source g_P and hence the power spectrum $\mathcal{P}_\mathcal{R}$ and its derivatives. Nevertheless, g_B can be explicitly connected to $\mathcal{P}_\mathcal{R}$ if we focus our attention on the case in which the most important source of features is specified. An example is given in [8] – a varying c_s gives rise to g_B that has the same origin as g_P, so we can specify the correlation. The same formula for $B_\mathcal{R}$ can be derived using the GSR approximation [10].

Another typical and important case is when the inflaton potential $V(\phi)$ exhibits sudden changes, such as kinks and steps[1] [16, 17]. In that case, with $c_s = 1$, the dominant source of the features is the variation of ϵ, i.e. $\eta \equiv \dot\epsilon/(H\epsilon)$ provided that inflation is not disturbed even with a violent variation of ϵ because $\epsilon \ll 1$ at all times. Then, GSR is a powerful tool to provide analytic results for the power spectrum [18] as well as the bispectrum [13], which would otherwise require time-intensive numerical calculations [20, 19,5]. The usual cubic action [14] is, however, not appropriate because a term with η is contained in the field redefinition, which we should later restore by hand. It is thus desirable to use an alternative form where η is explicit outside the field redefinition terms. This form is presented in [21], and collecting only terms with η,

$$S_3 \supset \int d^4x a^3 \epsilon m_{\mathrm{Pl}}^2 \left[-\eta\dot{\mathcal{R}}^2\mathcal{R} + \frac{\eta}{a^2}\mathcal{R}(\nabla\mathcal{R})^2\right].\tag{2}$$

To compute the bispectrum it is convenient, since $\epsilon \ll 1$, to consider a perfect de Sitter background $\tau = -1/(aH)$. Then η can be written to leading order in GSR as

$$\eta = -\int_0^\infty \frac{dk}{k} m(-k\tau) \frac{d\log\mathcal{P}_\mathcal{R}}{d\log k}.\tag{3}$$

Plugging this expression into (2) with the fluctuations given by the de Sitter mode functions, we derive an alternative form to [8] connecting the bispectrum with the power spectrum and its first two derivatives:

$$B_\mathcal{R}(k_1, k_2, k_3)$$
$$= \frac{(2\pi)^4\mathcal{P}_\mathcal{R}^2}{(k_1 k_2 k_3)^3}\left\{\int_{K/2}^\infty dk(n_\mathcal{R} - 1)\frac{\Delta^2}{k^2} + \left[\left(k_1^2 + k_2^2 + k_3^2\right)\right.\right.$$

$$\times \frac{k_1 k_2 + k_2 k_3 + k_3 k_1}{16k} + \frac{(k_1 k_2)^2 + (k_2 k_3)^2 + (k_3 k_1)^2}{8k}$$
$$\left.- \frac{k_1 k_2 k_3}{8}\right](1 - n_\mathcal{R}) + \frac{k_1 k_2 k_3}{8}\alpha_\mathcal{R}\right\},\tag{4}$$

where $\mathcal{P}_\mathcal{R} = H^2/\left(8\pi^2\epsilon m_{\mathrm{Pl}}^2\right)$ is the featureless flat power spectrum and the right hand side is evaluated at $k = (k_1 + k_2 + k_3)/2 \equiv K/2$. Here, $\Delta^2 = K(K - 2k_1)(K - 2k_2)(K - 2k_3)/16$ is the area squared of the triangle with three sides k_1, k_2 and k_3. Furthermore, with the f_{NL} ansatz [22] in mind, we may define a dimensionless shape function

$$f_{\mathrm{NL}}(k_1, k_2, k_3) \equiv \frac{10}{3}\frac{k_1 k_2 k_3}{k_1^3 + k_2^3 + k_3^3}\frac{(k_1 k_2 k_3)^2 B_\mathcal{R}}{(2\pi)^4\mathcal{P}_\mathcal{R}^2}.\tag{5}$$

This can be evaluated in any configuration of interest. In particular, we can reproduce the standard consistency relation in the squeezed limit, say, $k_3 \ll k_1 \approx k_2$,

$$f_{\mathrm{NL}} = \frac{5}{12}(1 - n_\mathcal{R}),\tag{6}$$

for (4). Note that (4) is in agreement with the result of [23], where using a different method this formula was derived with the Δ^2 and $k_1 k_2 k_3(1 - n_\mathcal{R})/8$ terms missing on the grounds that they are subleading and do not contribute in the squeezed limit.

Before applying (4) to actual data, we have tested the veracity of GSR using a step potential [17,20]

$$V(\phi) = \frac{1}{2}m^2\phi^2\left[1 + \alpha\tanh\left(\frac{\phi - \phi_0}{\Delta\phi}\right)\right].\tag{7}$$

To this end, we numerically calculated the bispectrum using BINGO [19] and compared it with the output of (4). The results are shown in Fig. 1, from which we observe excellent agreement, for parameters of the potential such that $\epsilon \ll 1$ and $\eta \lesssim 1$. Thus using GSR, if $\mathcal{P}_\mathcal{R}$ can be estimated independently of any specific inflationary model, one can make general statements regarding the location and magnitude of any potentially observable features in the bispectrum. However, for sharper departures from slow-roll, where one expects slow-roll parameters to be greater than unity, our leading-order analytic approximation starts deviating from the exact solution[2] and numerical computations such as BINGO can provide the accurate results. Finally note that we can use analytic templates as well to model sharp features like steps [17].

3. Bispectrum reconstruction from power spectrum

Reconstruction of the primordial power spectrum using the CMB temperature data has been the subject of considerable research over the past decade. Here we adopt the model-independent, non-parametric modified Richardson–Lucy algorithm [4,5], which relates $\mathcal{P}_\mathcal{R}$ in k-space to the CMB temperature power spectrum $\mathcal{C}_\ell$ using a convolution of the form

$$\mathcal{C}_\ell = \sum_i G_{\ell k_i}\mathcal{P}_{k_i},\tag{8}$$

where $G_{\ell k_i}$ is the radiative transport kernel that contains information regarding the background cosmology and i denotes the discrete k-space binning index. $\mathcal{C}_\ell$ is obtained using the 2013 release of Planck temperature data [24], in which we use four frequency channels covering a multipole range $2 \leq \ell \leq 2500$. The removal of

---

[1] In a recent article [25] a one-parameter formula for the correlation of the bispectrum and the power spectrum has been derived for the case of both a non-trivial sound speed and potential features upon certain assumptions.

[2] See [13] for complementary results, where next-to-leading order GSR corrections are shown to improve the bispectrum estimate for sharper departures from slow-roll.
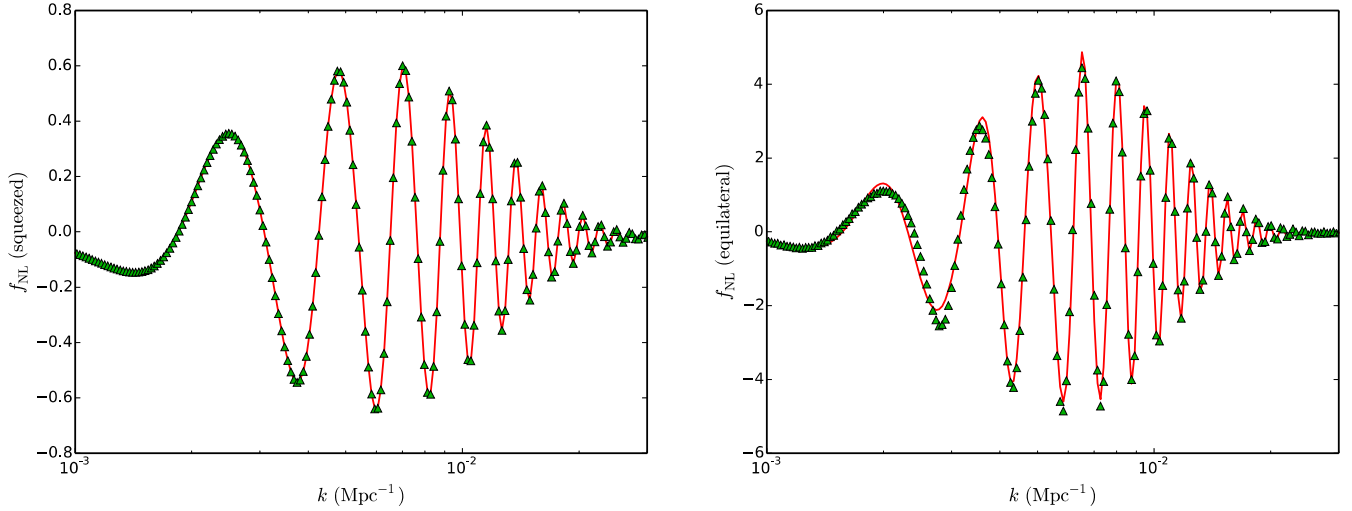
Fig. 1. The f_{NL} parameter (5) in the (left) squeezed and (right) equilateral limit for the inflationary model (7). Solid lines indicate f_{NL} calculated by full numerical evaluation using BINGO, and triangles correspond to the GSR calculation (5).
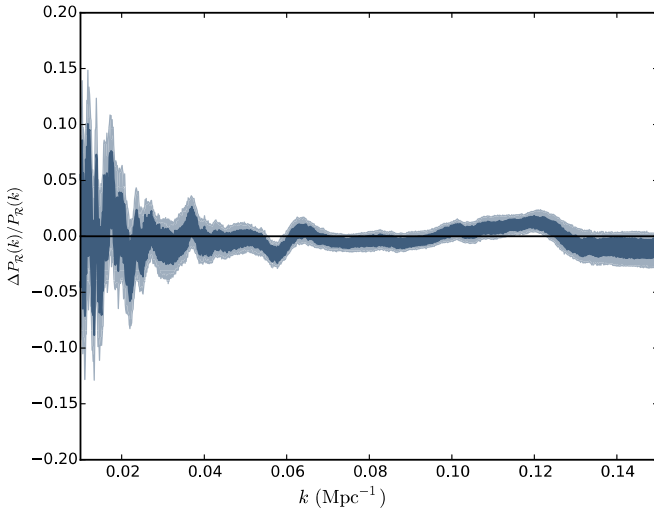

Fig. 2. A model-independent reconstruction of $\mathcal{P}_\mathcal{R}(k)$ according to the procedure outlined in the text. Here we plot the fractional deviation with respect to the best fit power-law model. The dark (light) shaded contours contain 68% (95%) of the reconstructed $\mathcal{P}_\mathcal{R}(k)$.

foregrounds and lensing, and the iterative procedure by which (8) is inverted to obtain $\mathcal{P}_\mathcal{R}(k)$ along with all details pertaining to the reconstruction method can be found in [5].

The recovered $\mathcal{P}_\mathcal{R}(k)$ possesses both features and unavoidable noise. Indeed one cannot make a clear distinction between them when using a model-independent reconstruction. However, the important point for our purposes is that the shape of the resulting $\mathcal{P}_\mathcal{R}(k)$ is independent of any specific inflationary model, and the location of any significant deviations from a featureless power spectrum can direct our search for corresponding features in the bispectrum.

We generate $N_{real} = 1000$ Gaussian realizations of $\mathcal{C}_\ell$. They are obtained by taking the existing data points and adding Gaussian random fluctuations with variance equal to the diagonal component of the full error covariance matrix. Each $\mathcal{C}_\ell$ is then passed through the iterative procedure outlined in [5] to obtain a corresponding realization of $\mathcal{P}_\mathcal{R}(k)$. Following this they are smoothed with a Gaussian filter, and the resulting $\mathcal{P}_\mathcal{R}(k)$ provides an improved fit compared to the baseline model. The result is exhibited in Fig. 2. As reported in [5], we find the maximum deviation from

a featureless power spectrum lying at $k \sim 0.06$ Mpc^{-1} (the other feature near $k \sim 0.12$ Mpc^{-1} was reported to be a systematic error in Planck).

We now take the $N_{real} = 1000$ reconstructed $\mathcal{P}_\mathcal{R}$'s and estimate their bispectra using (4). To do so, we must numerically calculate the first and second derivatives of $\mathcal{P}_\mathcal{R}(k)$. This is achieved by constructing a Chebyshev spline to approximate a smooth continuous curve using i points. We use N_{Cheb} Chebyshev polynomials, where N_{Cheb} is an integer that dictates the smoothness of the splined curve. We choose N_{Cheb} such that the curve provides an equal χ^2 fit to the Planck temperature data as the non-parametric reconstruction. Based on this criteria, we choose a value of $N_{Cheb} = 1000$: a smaller value degrades the fit, resulting in a larger χ^2 and a curve that fails to capture the important features in the data, whereas a larger value introduces spurious oscillations that amount to capturing the noise.

Differentiating the Chebyshev fit, we calculate the bispectrum and exhibit f_{NL} given by (5) projected onto certain configurations in Fig. 3. In the squeezed configuration, there is a mild anomalous behaviour at $k \sim 0.06$ Mpc^{-1}, the same k-value for which the power spectrum exhibits a potential feature, however the amplitude of this deviation from a featureless bispectrum is very small. There is a larger amplitude discrepancy at $k \sim 0.014$ Mpc^{-1}.

In the equilateral limit, the shaded region is larger than in the squeezed limit. This is expected as $\alpha_\mathcal{R} = d^2 \log \mathcal{P}_\mathcal{R}/d \log k^2$ is no longer suppressed for this triangular configuration. Here the bispectrum corresponding to a flat, featureless power spectrum lies within the 95% bounding region for practically all k. There are some oscillations, however these are likely to represent noise in the fitting procedure. We arrive at this conclusion by varying N_{Cheb} over $N_{Cheb} = (800, 1200)$: all N_{Cheb} in this range provide a roughly comparable fit to the data and the oscillations are not robust to varying N_{Cheb}.

Given that we can reconstruct f_{NL} for any configuration, we can perform a general search in (k_1, k_2, k_3) space for regions with significant deviations from the flat $\mathcal{P}_\mathcal{R}$ expectation. We focus on k-bands which are known to possess a feature in $\mathcal{P}_\mathcal{R}$. Specifically, we fix, say, $k_1 = 0.06$ Mpc^{-1}, and explore the residual two-dimensional (k_2, k_3) subspace. We are especially interested in any regions where the featureless expectation value of f_{NL} lies outside the 95% bounded region of the reconstruction. Hence for each point in the (k_2, k_3) space, we calculate f_{NL}^{fid}, $f_{NL}^{+2\sigma}$ and $f_{NL}^{-2\sigma}$,
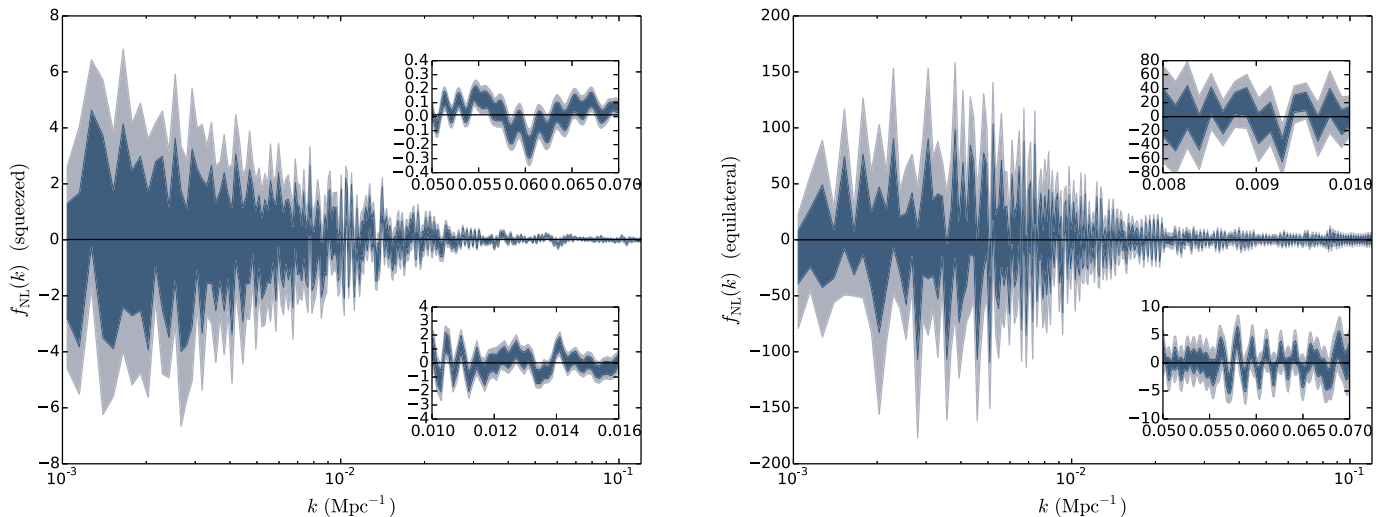
Fig. 3. f_{NL} in the (left) squeezed and (right) equilateral limit. The dark (light) band encloses 68% (95%) of the reconstructed $\mathcal{P}_{\mathcal{R}}$. The plot covers the entire range considered in this work, $k = (10^{-3}, 0.12)$ Mpc^{-1}. The inset plots exhibit certain k-bands of interest.
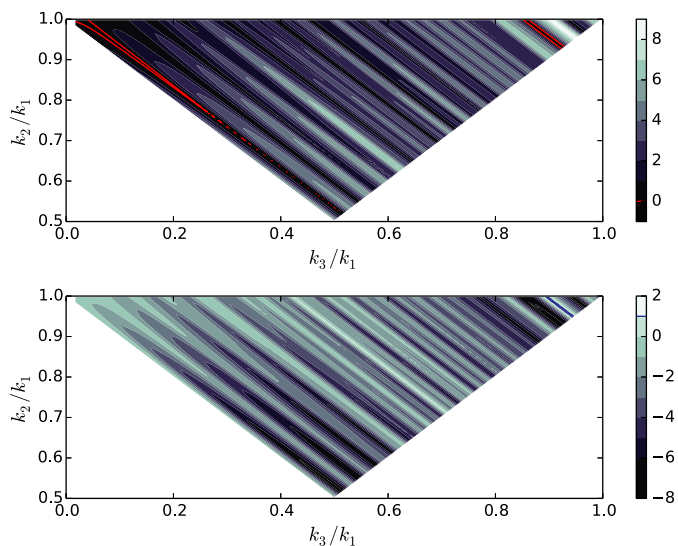

Fig. 4. Heat maps of $f_{\mathrm{NL}}^{+2\sigma} - f_{\mathrm{NL}}^{\mathrm{fid}}$ (top) and $f_{\mathrm{NL}}^{-2\sigma} - f_{\mathrm{NL}}^{\mathrm{fid}}$ (bottom) as a function of k_3/k_1 and k_2/k_1, with $k_1 = 0.06$ Mpc^{-1}. Regions of interest are $f_{\mathrm{NL}}^{+2\sigma} - f_{\mathrm{NL}}^{\mathrm{fid}} < 0$ and $f_{\mathrm{NL}}^{-2\sigma} - f_{\mathrm{NL}}^{\mathrm{fid}} > 0$, red (blue) contours in the top (bottom) panel, indicating areas where the featureless expectation value lies outside the 95% contours. (For interpretation of the references to color in this figure legend, the reader is referred to the web version of this article.)

where $f_{\mathrm{NL}}^{\mathrm{fid}}$ is the fiducial value of f_{NL}, calculated for a featureless $\mathcal{P}_{\mathcal{R}}$ with $n_{\mathcal{R}} = 0.96$, and $f_{\mathrm{NL}}^{+2\sigma}$, $f_{\mathrm{NL}}^{-2\sigma}$ are the values that bound 95% of the reconstructed f_{NL} from above and below. In Fig. 4 we show $f_{\mathrm{NL}}^{+2\sigma} - f_{\mathrm{NL}}^{\mathrm{fid}}$ and $f_{\mathrm{NL}}^{-2\sigma} - f_{\mathrm{NL}}^{\mathrm{fid}}$, plotting over the range $k_2/k_1 = (0.5, 1.0)$ and $k_3/k_1 = (10^{-3}, 1)$.

The stripes correspond to oscillations in f_{NL} observed in Fig. 3. Of particular interest are regions where $f_{\mathrm{NL}}^{+2\sigma} - f_{\mathrm{NL}}^{\mathrm{fid}} < 0$ and $f_{\mathrm{NL}}^{-2\sigma} - f_{\mathrm{NL}}^{\mathrm{fid}} > 0$. These are the regions where the featureless f_{NL} lies outside the 95% band, indicating possible features. They are exhibited as red (blue) contours in the top (bottom) panel of Fig. 4. Such behaviour is most clearly observed in the top left corner of the top panel in Fig. 4, i.e. most pronounced in the squeezed limit. There are a small number of narrow oscillatory bands which deviate from the featureless limit, however this is likely the same manifestation of noise as found in the equilateral configuration.

4. Conclusion

In this article we search for features in the bispectrum using the primordial power spectrum reconstructed from the angular power spectrum data of CMB temperature anisotropies. This is an important first step in extracting CMB three-point correlations directly from CMB two-point correlations of temperature fluctuations. The method presented is novel and allows a fast and reliable joint analysis of the CMB two- and three-point data. A model-independent reconstruction of the power spectrum can highlight the presence of features that we would expect to see in the bispectrum, and avoid model comparison with the data using a full Markov Chain Monte Carlo analysis.

Using our method, we find that in the squeezed configuration around $k \sim 0.014$ Mpc^{-1} and $k \sim 0.06$ Mpc^{-1} there are potential features with marginal 2σ confidence. In the equilateral configuration, the reconstructions do not strongly constrain the form of the bispectrum – a featureless bispectrum is consistent but we cannot rule out the possibility of large features being present.

Given the large uncertainty, it is important to confront these findings with CMB three-point temperature correlations directly. A joint constraint on inflationary features using the two- and three-point correlations of temperature [7] and polarization anisotropies is the best possible approach to find or alternatively rule out features with high confidence.

Acknowledgements

References

[1] A.H. Guth, Phys. Rev. D 23 (1981) 347;
A.D. Linde, Phys. Lett. B 108 (1982) 389;
A. Albrecht, P.J. Steinhardt, Phys. Rev. Lett. 48 (1982) 1220.

[2] See e.g D. Baumann, L. McAllister, arXiv:1404.2601 [hep-th].

[3] S.L. Bridle, A.M. Lewis, J. Weller, G. Efstathiou, Mon. Not. R. Astron. Soc. 342 (2003) L72, arXiv:astro-ph/0302306;
A. Shafieloo, T. Souradeep, P. Manimaran, P.K. Panigrahi, R. Rangarajan, Phys. Rev. D 75 (2007) 123502, arXiv:astro-ph/0611352;
D.K. Hazra, A. Shafieloo, G.F. Smoot, J. Cosmol. Astropart. Phys. 1312 (2013) 035, arXiv:1310.3038 [astro-ph.CO];
P. Hunt, S. Sarkar, arXiv:1510.03338 [astro-ph.CO].

[4] A. Shafieloo, T. Souradeep, Phys. Rev. D 70 (2004) 043523, arXiv:astro-ph/0312174;
D.K. Hazra, A. Shafieloo, T. Souradeep, J. Cosmol. Astropart. Phys. 1307 (2013) 031, arXiv:1303.4143 [astro-ph.CO].

[5] D.K. Hazra, A. Shafieloo, T. Souradeep, J. Cosmol. Astropart. Phys. 1411 (11) (2014) 011, arXiv:1406.4827 [astro-ph.CO].

[6] For previous studies, see e.g A. Achúcarro, V. Atal, P. Ortiz, J. Torrado, Phys. Rev. D 89 (10) (2014) 103006, arXiv:1311.2552 [astro-ph.CO];
A. Achucarro, V. Atal, B. Hu, P. Ortiz, J. Torrado, Phys. Rev. D 90 (2) (2014) 023511, arXiv:1404.7522 [astro-ph.CO];
J.R. Fergusson, H.F. Gruetjen, E.P.S. Shellard, M. Liguori, Phys. Rev. D 91 (2) (2015) 023502, arXiv:1410.5114 [astro-ph.CO].

[7] See also P.D. Meerburg, M. Münchmeyer, B. Wandelt, Phys. Rev. D 93 (4) (2016) 043536, arXiv:1510.01756 [astro-ph.CO].

[8] A. Achucarro, J.O. Gong, G.A. Palma, S.P. Patil, Phys. Rev. D 87 (12) (2013) 121301, arXiv:1211.5619 [astro-ph.CO].

[9] A. Achucarro, J.O. Gong, S. Hardeman, G.A. Palma, S.P. Patil, Phys. Rev. D 84 (2011) 043502, arXiv:1005.3848 [hep-th];
A. Achucarro, J.O. Gong, S. Hardeman, G.A. Palma, S.P. Patil, J. Cosmol. Astropart. Phys. 1101 (2011) 030, arXiv:1010.3693 [hep-ph];
A. Achucarro, J.O. Gong, S. Hardeman, G.A. Palma, S.P. Patil, J. High Energy Phys. 1205 (2012) 066, arXiv:1201.6342 [hep-th].

[10] J.O. Gong, K. Schalm, G. Shiu, Phys. Rev. D 89 (6) (2014) 063540, arXiv:1401.4402 [astro-ph.CO].

[11] E.D. Stewart, Phys. Rev. D 65 (2002) 103508, arXiv:astro-ph/0110322;
J. Choe, J.-O. Gong, E.D. Stewart, J. Cosmol. Astropart. Phys. 0407 (2004) 012, arXiv:hep-ph/0405155.

[12] M. Joy, E.D. Stewart, J.-O. Gong, H.-C. Lee, J. Cosmol. Astropart. Phys. 0504 (2005) 012, arXiv:astro-ph/0501659;
M. Joy, E.D. Stewart, J. Cosmol. Astropart. Phys. 0602 (2006) 005, arXiv:astro-ph/0511206.

[13] P. Adshead, W. Hu, C. Dvorkin, H.V. Peiris, Phys. Rev. D 84 (2011) 043519, arXiv:1102.3435 [astro-ph.CO];
P. Adshead, C. Dvorkin, W. Hu, E.A. Lim, Phys. Rev. D 85 (2012) 023531, arXiv:1110.3050 [astro-ph.CO];
P. Adshead, W. Hu, Phys. Rev. D 85 (2012) 103531, arXiv:1203.0012 [astro-ph.CO];
P. Adshead, W. Hu, V. Miranda, Phys. Rev. D 88 (2) (2013) 023507, arXiv:1303.7004 [astro-ph.CO].

[14] J.M. Maldacena, J. High Energy Phys. 0305 (2003) 013, arXiv:astro-ph/0210603;
D. Seery, J.E. Lidsey, J. Cosmol. Astropart. Phys. 0506 (2005) 003, arXiv:astro-ph/0503692;
X. Chen, M.x. Huang, S. Kachru, G. Shiu, J. Cosmol. Astropart. Phys. 0701 (2007) 002, arXiv:hep-th/0605045;
J. Martin, L. Sriramkumar, J. Cosmol. Astropart. Phys. 1201 (2012) 008, arXiv:1109.5838 [astro-ph.CO].

[15] C. Cheung, P. Creminelli, A.L. Fitzpatrick, J. Kaplan, L. Senatore, J. High Energy Phys. 0803 (2008) 014, arXiv:0709.0293 [hep-th].

[16] A.A. Starobinsky, JETP Lett. 55 (1992) 489, Pis'ma Zh. Eksp. Teor. Fiz. 55 (1992) 477.

[17] J.A. Adams, B. Cresswell, R. Easther, Phys. Rev. D 64 (2001) 123514, arXiv:astro-ph/0102236;
L. Covi, J. Hamann, A. Melchiorri, A. Slosar, I. Sorbera, Phys. Rev. D 74 (2006) 083509, arXiv:astro-ph/0606452;
D.K. Hazra, M. Aich, R.K. Jain, L. Sriramkumar, T. Souradeep, JCAP 1010 (2010) 008, arXiv:1005.2175 [astro-ph.CO];
V. Miranda, W. Hu, Phys. Rev. D 89 (8) (2014) 083529, arXiv:1312.0946 [astro-ph.CO].

[18] J.O. Gong, J. Cosmol. Astropart. Phys. 0507 (2005) 015, arXiv:astro-ph/0504383;
C. Dvorkin, W. Hu, Phys. Rev. D 81 (2010) 023518, arXiv:0910.2237 [astro-ph.CO];
W. Hu, Phys. Rev. D 84 (2011) 027303, arXiv:1104.4500 [astro-ph.CO].

[19] D.K. Hazra, L. Sriramkumar, J. Martin, J. Cosmol. Astropart. Phys. 1305 (2013) 026, arXiv:1201.0926 [astro-ph.CO];
V. Sreenath, D.K. Hazra, L. Sriramkumar, J. Cosmol. Astropart. Phys. 1502 (02) (2015) 029, arXiv:1410.0252 [astro-ph.CO].

[20] X. Chen, R. Easther, E.A. Lim, J. Cosmol. Astropart. Phys. 0706 (2007) 023, arXiv:astro-ph/0611645;
X. Chen, R. Easther, E.A. Lim, J. Cosmol. Astropart. Phys. 0804 (2008) 010, arXiv:0801.3295 [astro-ph].

[21] C. Burrage, R.H. Ribeiro, D. Seery, J. Cosmol. Astropart. Phys. 1107 (2011) 032, arXiv:1103.4126 [astro-ph.CO].

[22] E. Komatsu, D.N. Spergel, Phys. Rev. D 63 (2001) 063002, arXiv:astro-ph/0005036.

[23] G.A. Palma, J. Cosmol. Astropart. Phys. 1504 (04) (2015) 035, arXiv:1412.5615 [hep-th].

[24] P.A.R. Ade, et al., Planck Collaboration, Astron. Astrophys. 571 (2014) A15, arXiv:1303.5075 [astro-ph.CO].

[25] S. Mooij, G.A. Palma, G. Panotopoulos, A. Soto, J. Cosmol. Astropart. Phys. 1510 (10) (2015) 062, arXiv:1507.08481 [astro-ph.CO].